Braz J Phys (2016) 46:220–224
DOI 10.1007/s13538-016-0402-y

SOCIEDADE BRASILEIRA DE FÍSICA

PARTICLES AND FIELDS

Spreading Simulation of Droplet Impact on Solid Surface with CLSVOF Method and Its Experimental Verification

Yan-Jun Zhang[1] · **Ping Li**[1]

Received: 1 May 2015 / Published online: 3 February 2016

Abstract A coupled volume-of-fluid and level set (CLSVOF) method is applied for the simulation of droplet impacting on a solid surface. This two-phase flow approach combines the advantages of VOF and level set (LS) methods. Three cases are listed and simulated by CLSVOF method, and the wettability is evaluated by tracking the three-phase contact line (TPCL). Results showed that the change of liquid spreading ratio with time has a good fit with the experimental results of the above three cases and high accuracy is achieved by CLSVOF method compared with VOF method, which indicated that this model is suitable for researching the wetting problem. The spreading speed on good wettability surfaces is faster than that of on poor wettability surfaces significantly, and the recoiling phenomenon appears after the droplet spreading to its maximum.

Keywords Droplet · Impact · CLSVOF method · Contact line

1 Introduction

Wetting, as a typical free flow phenomenon on liquid surface, is ubiquitous in the industrial field of dust-fall wetting, coal seam water infusion, dying printing, spray cooling or nebulizers in medical use, etc. Wetting is a process of droplet spreading on solid surface, which is reflected by the three-phase contact line (TPCL) and the contact angle (AC) [1–11]. Yang (1805) is the first person who defined the concept of contact angle between water and solid surface [12], and then Cassie and Baxter (1936) characterized the trapping of air between a droplet and a rough surface [13]. Marmur (2003) considered a droplet partially wets the surface and partially sits on air pockets [14]. Researches on the fluid dynamics of droplet impact on a solid surface become more difficult due to the influence of the extreme deformation of a droplet in a short period of time and the presence of surface tension and viscosity. Generally, two phenomena may occur after a tiny droplet impacts on a solid surface at different velocities. When the impact velocity is low, the droplet may stand on the solid surface in a liquid form; when the impact velocity is fast, the droplet may splash and be split into smaller droplets [15–18]. In our study, splashing will not be mentioned.

From a theoretical point of view, the prediction of droplet impact on solid surface is difficult to make because of its unstable properties. In the earliest research, the influence of wettablity parameters on spreading process was observed by experiment, but it was difficult to obtain the microscopic behaviors [19, 20]. Harlow et al. [21] first suggested a fluid numerical model of droplet impingement on solid surfaces with ignorance of all surface tension and viscosity. After that, a couple of numerical approaches were proposed on the basis of approximation. Gao et al. [22] set up the molecular dynamics model of spreading process by using the moving particle semi-implicit method (MPS) and analyzed the micro-structure influence of solid-liquid interface on wettability. Yang et al. [23] simulated the droplet oscillation level during the impact process by using the CFD method with consideration of the shapes of droplet oscillation and internal flow induced by receding. Su et al. [24] presented a numerical simulation of a single liquid drop impacting onto solid surface with smoothed particle hydrodynamics (SPH), and the numerical results are in good agreement with the theoretical and experimental results. Liu et al. [25, 26] studied the dynamic behaviors of

✉ Yan-Jun Zhang
yjzhang222@126.com

[1] College of Mechanical Engineering, Taiyuan University of Science and Technology, Taiyuan 030024, China

droplet spreading on solid surface by using lattice Boltzmann method (LBM) coupled with spreading mechanics model and found that the spreading contact angle can be lower than 90° with the consumption that the droplet surface tension is small enough. Sun et al. [27] researched two-phase flow dynamics approach for micro droplet impacting on a flat dry surface by using VOF multiphase model to calculate the flow distributions and found this model fit the experimental data well.

In this paper, we established a numerical simulation of droplet wetting phenomenon by using a coupled volume-of-fluid and level set (CLSVOF) method, which combines the advantages of VOF and level set (LS) methods. Finally the computing results got by CLSVOF method are compared with the results from three other cases.

2 Droplet Impact Modeling

The evolution after droplet impact on solid surface is a complex two-phase flow process with interface deformation, making the simulation of droplet flow more difficult. The key problem is to capture the interface effectively. CLSVOF combines VOF and LS method, where LS function is used to compute the curvature and normal vector to the interface accurately while VOF function is used to reconstruct the interface. In this study, a two-phase flow approach employed by CLSVOF is a three-dimensional model which combines a fixed mesh discretization and the Navier–Stokes equations with a piecewise linear volume tracking algorithm to track the droplet free surface with ignorance of the heat transfer and solidification. The conditions of flow field are incompressible and isothermal, and the model is assumed as the following: (i) the value of dynamic AC depends on the velocity of TPCL; (ii) the advancing AC is larger than the receding AC; (iii) more than one values of AC are possible for a stationary contact line [26].

The continuity and Navier–Stokes equation can be given by Eqs. (1) and (2).

$$\nabla \vec{u} = 0 \tag{1}$$

Table 1 Detail conditions for three cases

	Case 1	Case 2	Case 3
Droplet diameter, D_0/mm	0.085	3.88	2.19
Initially velocity, V_0/(m/s)	5.1	2.698	0.517
Static contact angle, θ/(°)	35	8	10
Re	434	10,416	1130
We	30	387	8.2

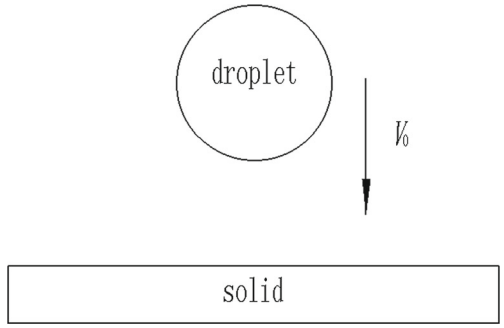

Fig. 1 Schematic of simulation cases

$$\frac{\rho \partial \vec{u}}{\partial t} + \rho \nabla \cdot \left(\vec{u}\,\vec{u} \right) = -\nabla p + \nabla \mu \left[\nabla \vec{u} + \left(\nabla \vec{u} \right)^T \right] - \sigma \kappa \delta(\phi) \nabla \phi + \rho g \tag{2}$$

Where ρ, p, σ are separately the liquid density, pressure, and surface tension; g is the gravity acceleration, κ is the interface curvature, which is calculated by the following equation:

$$\kappa = \nabla \cdot \frac{\nabla \phi}{|\nabla \phi|} \tag{3}$$

and $\delta(\phi)$ is the distance function confounded with the Dirac function and defined as:

$$\delta(\phi) = \begin{cases} \dfrac{1 + \cos\left(\pi \phi / a\right)}{2a} & |\phi| < a \\ 0 & |\phi| \geq a \end{cases} \tag{4}$$

where $a = 1.5w$ and w is the minimum size of the cell.

The interface normal vector $\vec{n}$ can be calculated by Eq. (5).

$$\vec{n} = \frac{\nabla \varphi}{|\nabla \varphi|} \tag{5}$$

When the moving interface is tracked, the cumulative of numerical dissipation will generate the interface profile vague or oscillations, so it is necessary to reconstruct the interface for each time step. Computing has been carried

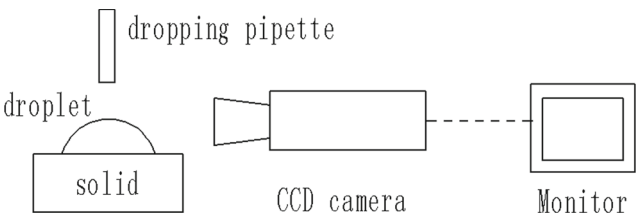

Fig. 2 Sketches of droplet impact experiment

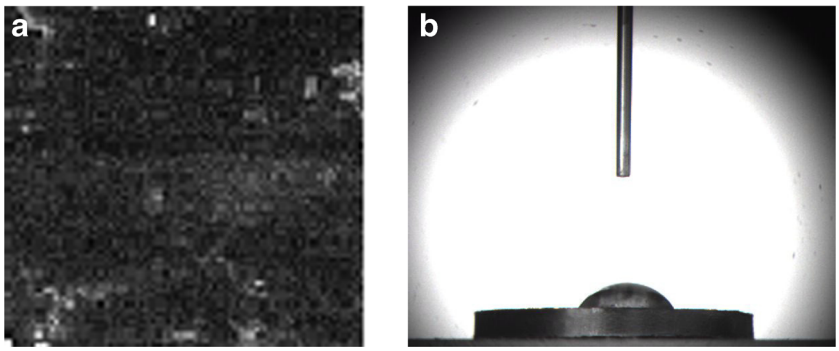

Fig. 3 Sem of solid surface (**a**) and droplet impact process (**b**)

on the different labor in the CLSVOF method; the VOF function provides the size of portion through which the interface may pass, and LS function determines the direction of the interface calculated by the interface normal vector though Eq. (5) [28]. TPCL needs to be treated carefully during the spreading process, and its velocity is calculated by Blake's model [29]. In this paper, we certified the accuracy of the model by comparing the three cases whose detail conditions are listed in Table 1. The dimensionless parameters *We*, *Re* are respectively defined as

$$\mathrm{Re} = \frac{V_o D_o}{\gamma}, \mathrm{We} = \frac{\rho D_o V_o^2}{\sigma} \tag{6}$$

where V_0 and D_0 are the initial velocity and diameter of droplet respectively, $.\gamma$ is dynamic viscosity.

A schematic of a droplet impact on solid surface is illustrated in Fig. 1 and the 2-d axisymmetric simulation was performed. The initial time is set just when the droplet contacts the solid surface. The mesh size equals 1/100 of the droplet diameter and is determined by a mesh refinement study. The grid spacing of mesh is gradually increased until further increments making no significant changes, and the mesh number 200×200 are determined eventually. The convective terms both in the Navier–Stokes equation and LS function are solved by quadratic upwind interpolation of convective kinematics; VOF and LS functions are solved by geo-reconstruction and MUSCL, respectively. The pressure and velocity are coupled by PISO. The time step used to compute is 0.05 μs. The calculation time ranges from 30 to 50 h for each case with four CPUs on a 64-bit Linux Cluster.

3 Droplet Impact Experiment

The test of droplet impact experiment is shown in Fig. 2, the FTA 200 system (First Ten Angstroms, USA), was used to capture the droplet spreading process and to record images every 0.1 s under the conditions of room temperature $20 \pm 2°$ and relative humidity 55 ± 3 %. The system consists of five parts: The CCD camera, monitor, dropping pipette, solid, and droplet. The CCD camera has a maximum speed of 30 frames per second; the monitor is used to display the image and the output results; the dropping pipette is used to control the falling height; the choosing of solid material is steel (Q235) whose surface electron microscopy (sem) is shown in (Fig. 3a); the droplet is water.

The typical images of a droplet impact on solid surface (Fig. 3b) were shown, and the contact angle was measured from the droplet profile using the FTA 200 software. Each experiment was repeated 10 to 20 times on each solid surface, and the data obtained were regarded to be acceptable only if for three repetitions. Due to the apparent contact angle was scatted in a range, we used an average value as the apparent contact angle in the curve-fitting process subsequently.

4 Results and Discussion

4.1 Comparation with Case 1

Liquid contour images can be obtained by tracking the movement of droplet surface unit, and Fig. 4 shows the contour change of droplet spreading on a solid surface under the parameters in Table 1 with the image time

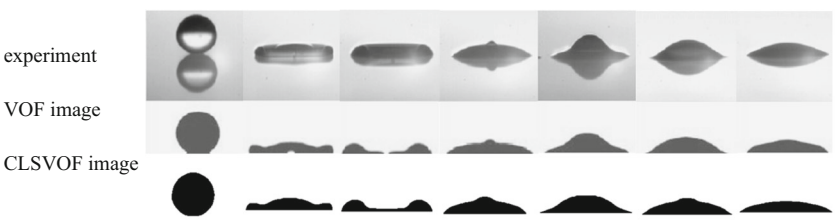

Fig. 4 Droplet evolution in case 1

interval 15 μs. When a droplet impacts on solid surface, it spreads radically until spreading diameter attains its maximum and forms a lamella. During the process, the shape of the droplet changes from a sphere to a disc-like appearance. Then, the droplet recoils and continues to spread at a rather low rate. At the end of the spreading process, it reaches an equilibrium state. At the moment, the free energy achieves its minimum value, the interface shape and contact line are no longer changing anymore, and the contact angle arrives at its static value. The static value of experiment, VOF and CLSVOF, respectively, are 32.25, 38.46, and 33.42°. So the result of CLSVOF is better than that of VOF under the experiment as a comparison standard.

We adopt the liquid spreading ratio β to measure the velocity of TPCL and define $\beta = D/D_0$, where D and D_0 are the liquid spread and initial diameter, respectively. Figure 5 shows the comparisons among CLSVOF simulation, VOF simulation [28] and experiment images for the change of contact angle in droplet spreading on solid surface, where R^2 is used to evaluate the goodness of curve fit. The R^2 of CLSVOF and VOF corresponded to the experimental dates are 0.99 and 0.97, respectively, which indicates the goodness of curve fit between CLSVOF simulation and experiment is better than that of VOF.

The oscillations induced by the poor wettability of surface are discovered in the whole spreading process, especially at the final stage, and it is believed that the obvious oscillations in experiment is in connection with test environment [17]. It is noticed that β reduces after droplet spreading to the maximum, namely the curve slope down a little, which is shown in Fig. 4. After droplet recoiling, the value of CLSVOF is closer to the experimental data compared with VOF, which further certificates the feasibility of CLSVOF to deal with the liquid free flow issue.

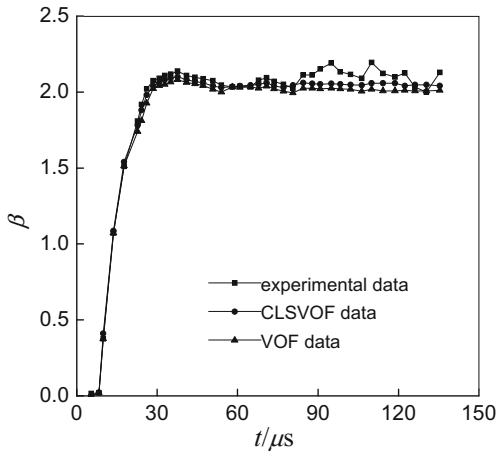

Fig. 5 Comparison of spreading ratio curves with case 1

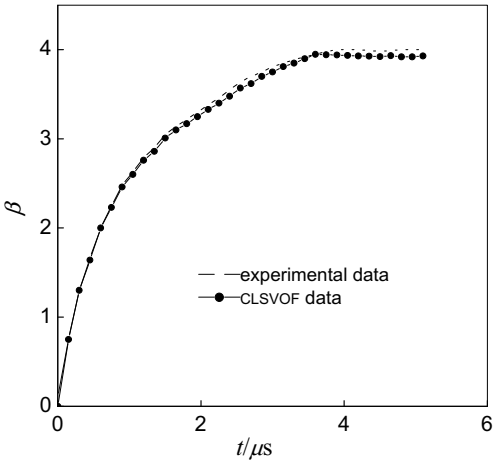

Fig. 6 Comparison of spreading ratio curves with case 2

4.2 Comparation with Case 2

Figure 6 shows the dynamic spreading comparison of droplet between CLSVOF simulation and the experimental results from case 2 with parameters in Table 1. Compared with Fig. 2, the total spreading time reduces to 1/26, which indicates that the better the wettability is, the faster the droplet spreads, and the same result is got in Ref. [26]. The R^2 from Fig. 4 is 0.99, which indicates a perfect match between simulation and experiment. By comparing the value of R^2, case 2 is a little larger than that of case 1, which may be caused by the poor effect of oscillation under good wettability surface. We can refer that the velocity of TPCL has much less influence on contact angle when droplet impacts on a good wettability surface, which is consistent with Ref. [28]. In Ref. [28], no recoiling was got due to good wettability, but we find that the curves slope down by CLSVOF method. By comparing with case 1, the curve changes gently due to good wettability, which indicates that the better the wettability is, the easier the droplet spreads.

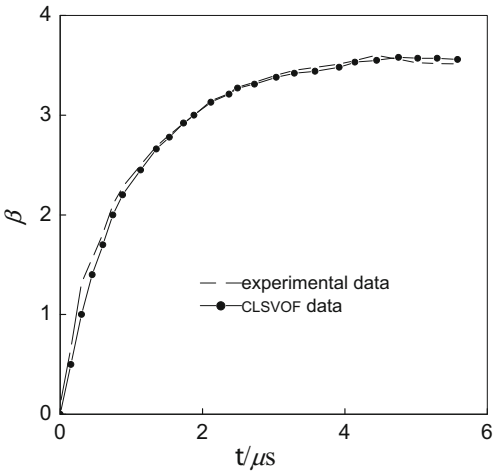

Fig. 7 Comparison of spreading ratio curves with case 3

4.3 Comparation with Case 3

The R^2 is 0.98 through the comparison between CLSVOF simulation and the results from case 3 in Fig. 7, which proves that the match between simulation and experiment perfect well. It is noticed that the initial spreading shows a great difference. The internal molecules of droplet have a severe oppression under the action of gravity at the initial spreading. When the initial velocity is low, the droplet viscosity plays a major role. The droplet viscosity performed in numerical method is set by the intermolecular forces, and the accumulative error calculated by each time step when the distance between molecules becomes closer. For solving this problem during the numerical process, the meshless method needs to introduce, which will be explained in our next study.

5 Summary

In this paper, we presented a novel model that coupled volume-of-fluid and level set (CLSVOF) method in the simulation of droplet impacting on solid surface without considering the heat transfer and solidification. The accuracy of this model was verified by comparing with three kinds of results. The study showed that the change of liquid spreading ratio with time by CLSVOF method has a good fit with the experimental results by the three cases, and the accuracy by using CLSVOF method is higher than that of by VOF method. The spreading speed on good wettability surfaces is significantly faster than on poor wettability surfaces, and the recoiling phenomena can appear after the droplet spreading to its maximum. For the initial spreading, the simulation prediction can be more accurate.

Acknowledgments The work described in this paper was supported by the Scientific Research Foundation for the Doctors of Taiyuan University of Science and Technology, China (Grant No. 20142038) and the University Science and Technology Innovation Project of Shanxi Province (Grant No. 2015170).

References

1. R.D. Narhe, D.A. Beysens, Langmuir **23**, 6486 (2007)
2. R.S. Mahmood, B. Sonia, G.F. Luc, Appl. Surf. Sci. **258**, 6416 (2012)
3. Q. Wei, Y.L. Ding, Z.R. Nie, X.G. Liu, Q.Y. Li, J Membr Sci **466**, 114 (2014)
4. R. Tsekova, D. Borissovb, S.I. Karakasheva, Colloids Surf A **423**, 77 (2013)
5. K.S. Lee, V.M. Starov, J. Colloid Interface Sci. **329**, 361 (2009)
6. G.W. Koen, H.W. Joost, E. Antonin, Phys. Rev. E **85**, 055301 (2012)
7. X. Feng, L. Feng, M. Jin, J. Zhai, L. Jiang, J. Am. Chem. Soc. **126**, 62 (2004)
8. T. Sun, G. Wang, L. Feng, B. Liu, Y. Ma, Chem Int Ed **43**, 357 (2004)
9. T.N. Krupenkin, J.A. Taylor, E.N. Wang, P. Kolodner, P. Hodes, Langmuir **23**, 9128 (2007)
10. R.D. Nahre, D.A. Beysens, Phys. Rev. Lett. **93**, 076103 (2004)
11. Y.T. Cheng, D.E. Rodak, Appl. Phys. Lett. **86**, 144101 (2005)
12. T. Young, Philos. Trans. R. Soc. Lond. **94**, 1 (1805)
13. R.N. Wenzel, Ind Eng Chem **8**, 988 (1936)
14. A. Marmur, Langmuir **20**, 8343 (2003)
15. S.L. Manzello, J.C. Yang, Exp. Fluids **32**, 580 (2002)
16. P.F. Hao, C.J. Lv, Z.H. Yao, Europhys. Lett. **90**, 66003 (2010)
17. Q.Z. Liu, Z.M. Kou, Z.N. Han, J. Cent. South Univ. **08**, 3247 (2014)
18. S.S. Liu, C.H. Zhang, H.B. Zhang, J. Zhou, Chin Phys B **22**, 106801 (2013)
19. J.C. Douglas, N.C. Gomes, R.S. Josmary, Measurement **46**, 3623 (2013)
20. M.K. John, L.H. Nicholas, D. Murat, Exp. Thermal Fluid Sci. **54**, 179 (2014)
21. F.H. Harlow, J.P. Shannon, J. Appl. Phys. **38**, 3855 (1967)
22. Y.F. Gao, Y. Yang, D.Y. Sun, Chin. Phys. Lett. **28**, 036102 (2011)
23. J. Yang, Z.Z. Zhang, X.H. Men, X.H. Xu, X.T. Zhu, Carbon **49**, 19 (2011)
24. T.X. Su, L.Q. Ma, M.B. Liu, J.Z. Chang, Acta Phys. Sin. **62**, 064702 (2013)
25. Q.Z. Liu, Z.M. Kou, Z.N. Han, Acta Phys. Sin. **62**, 234701 (2013)
26. Q.Z. Liu, Z.M. Kou, Y.M. Jia, Acta Phys. Sin. **10**, 304 (2014)
27. F.X. Sun, J.F. Wang, Y.M. Cheng, Chin Phys B **22**, 120203 (2013)
28. Y.L. Guo, L. Wei, G.T. Liang, S.Q. Shen, Int Commun Heat Mass **53**, 26 (2014)
29. A. Albadawi, D.B. Donoghue, A.J. Robinson, D.B. Murray, Int J Multiphase Flow **53**, 11 (2013)